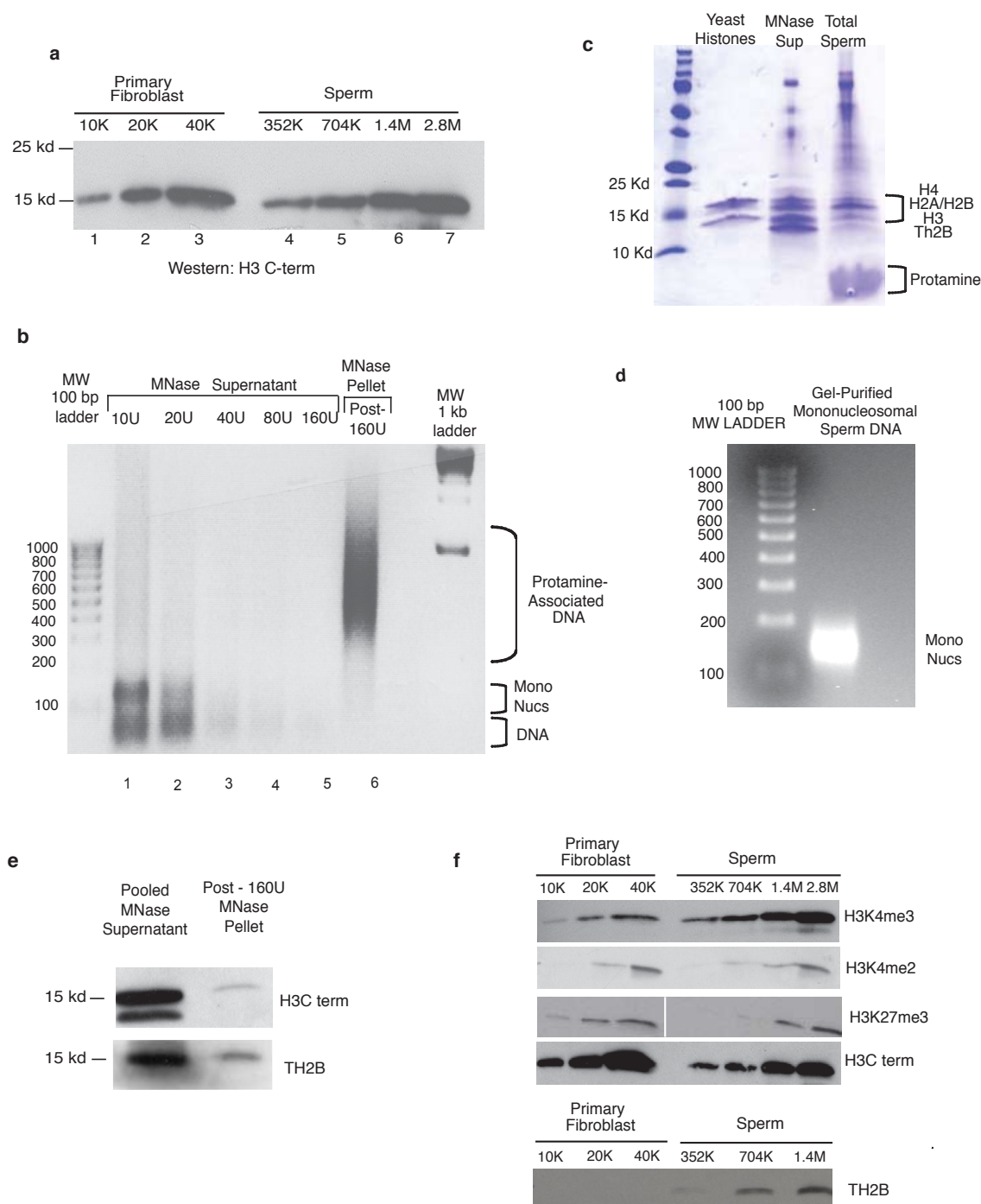
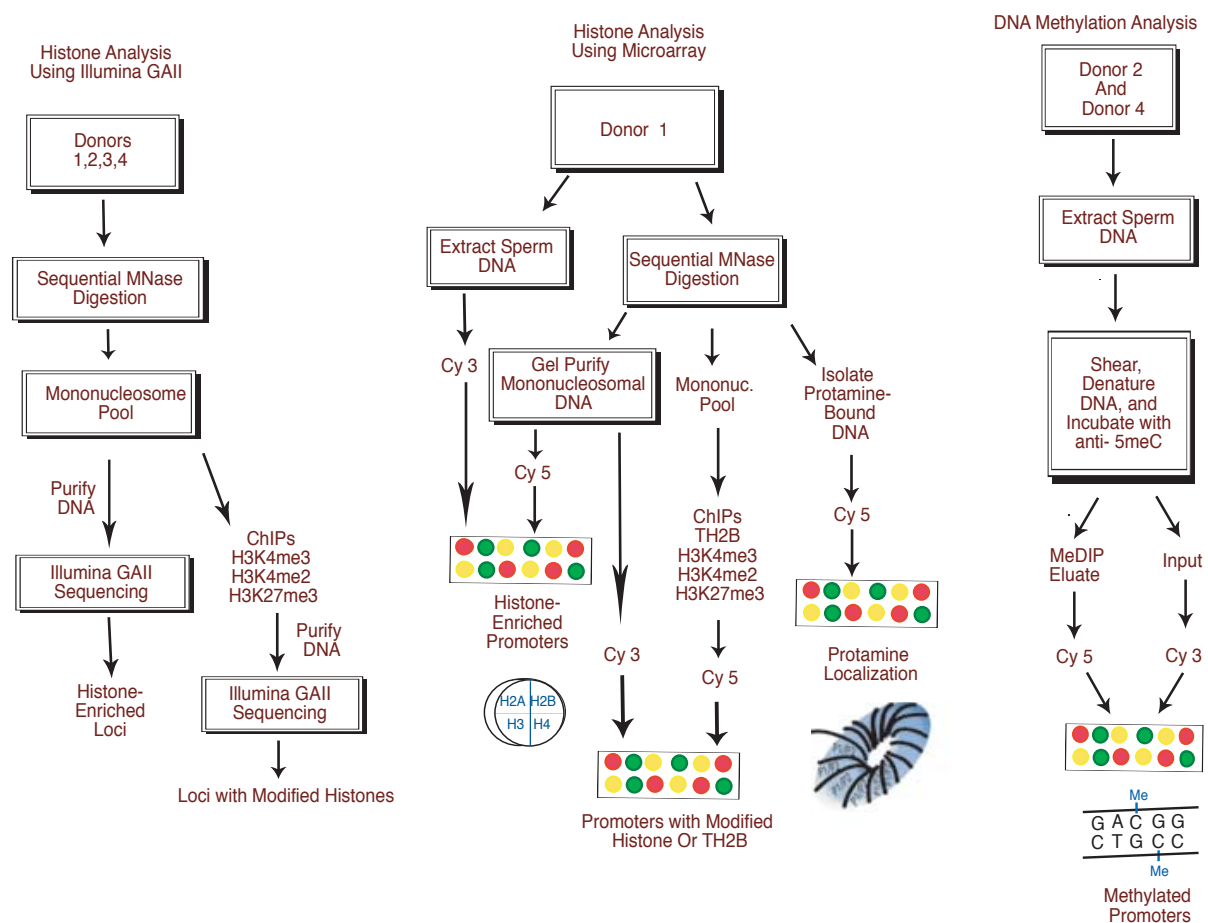


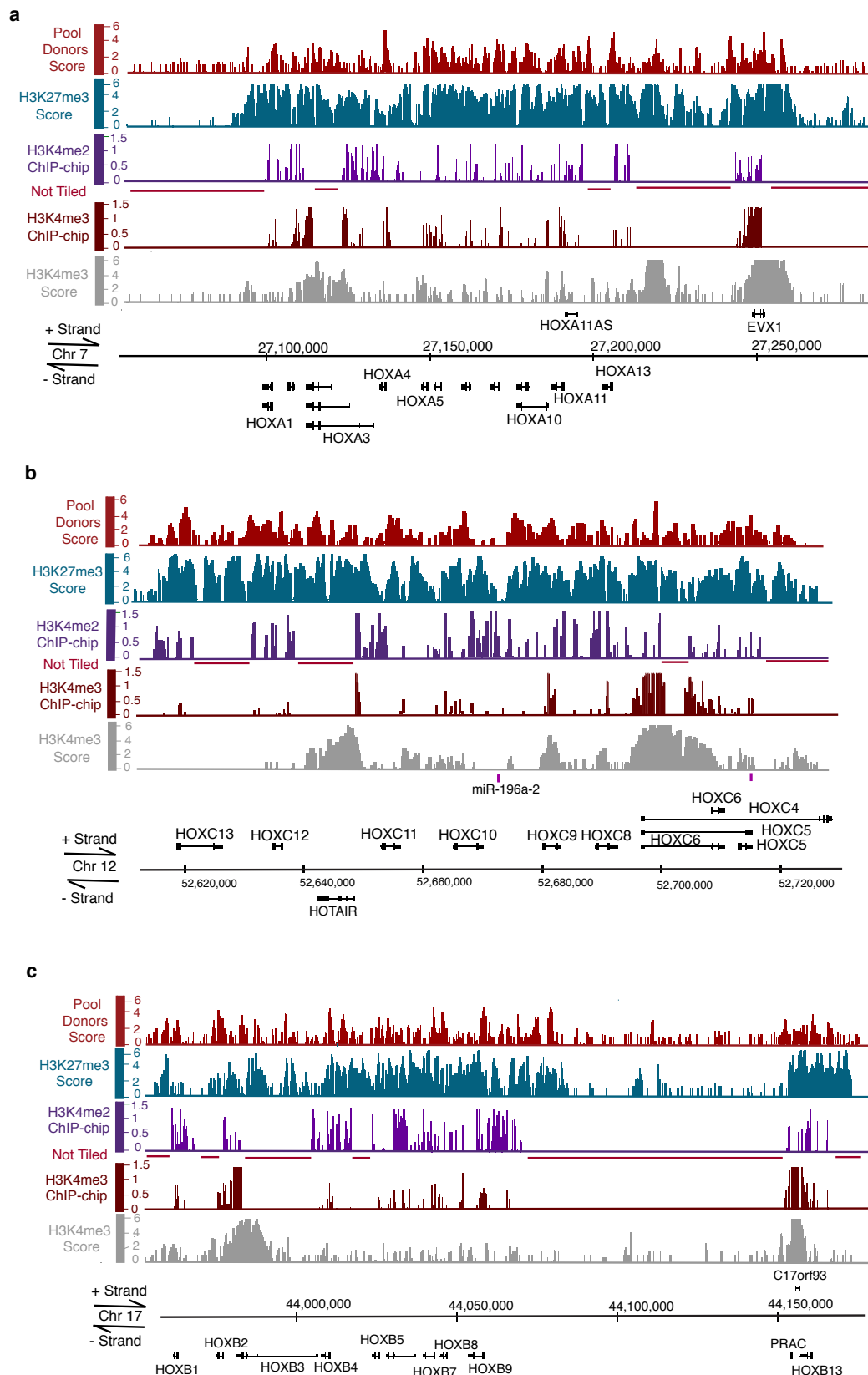
SUPPLEMENTARY INFORMATION



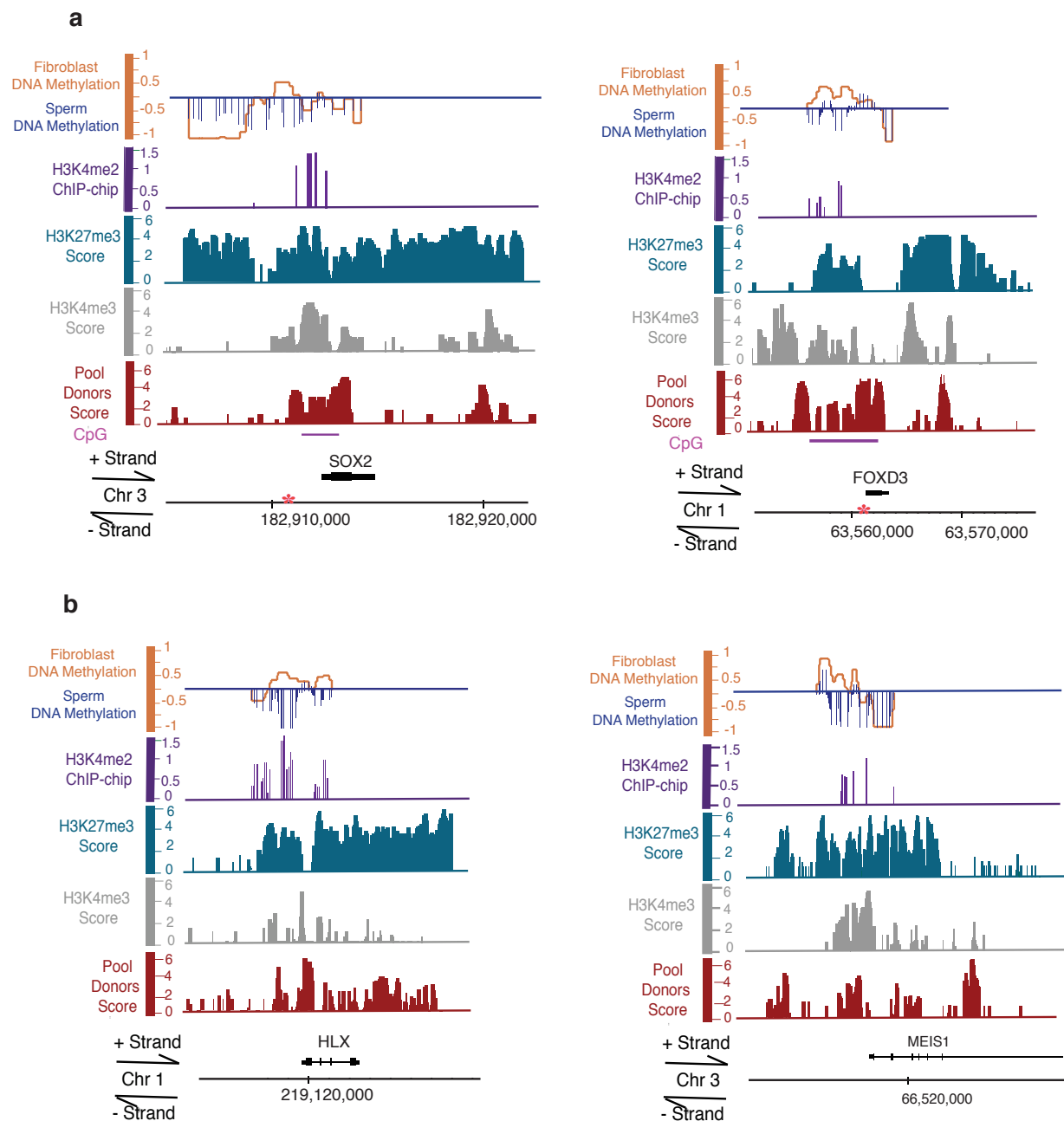
Supplemental Fig. 1: Composition of human sperm chromatin. **a**, Quantifying histone content of primary fibroblast or human sperm cells by immunoblot analysis with the H3C terminus antibody. **b**, Sequential digestion of sperm chromatin with increasing concentrations of micrococcal nuclease (MNase) releases mononucleosomes (lanes 1 and 2), whereas protamine-packaged chromatin resists MNase (lane 6). **c**, Characterizing the mononucleosome fraction released into the MNase supernatant pool from panel **b**. **d**, Gel-purified mononucleosomal DNA used for array hybridization or sequencing. **e**, Quantification of the amount of histone released by MNase treatment. Supernatants were pooled. Here, cell equivalents were loaded in each lane; 4% of the total supernatant or protamine pellet. The gel was subjected to immunoblotting and quantified on a Typhoon (Amersham). **f**, Western analysis, involving titrations for bulk levels of H3K4me3, H3K4me2, H3K27me3 in primary fibroblast cells and mature sperm cells. Quantitation by Typhoon (Amersham) reveals that sperm bear ~4% of the histone H3 present in a primary fibroblast.



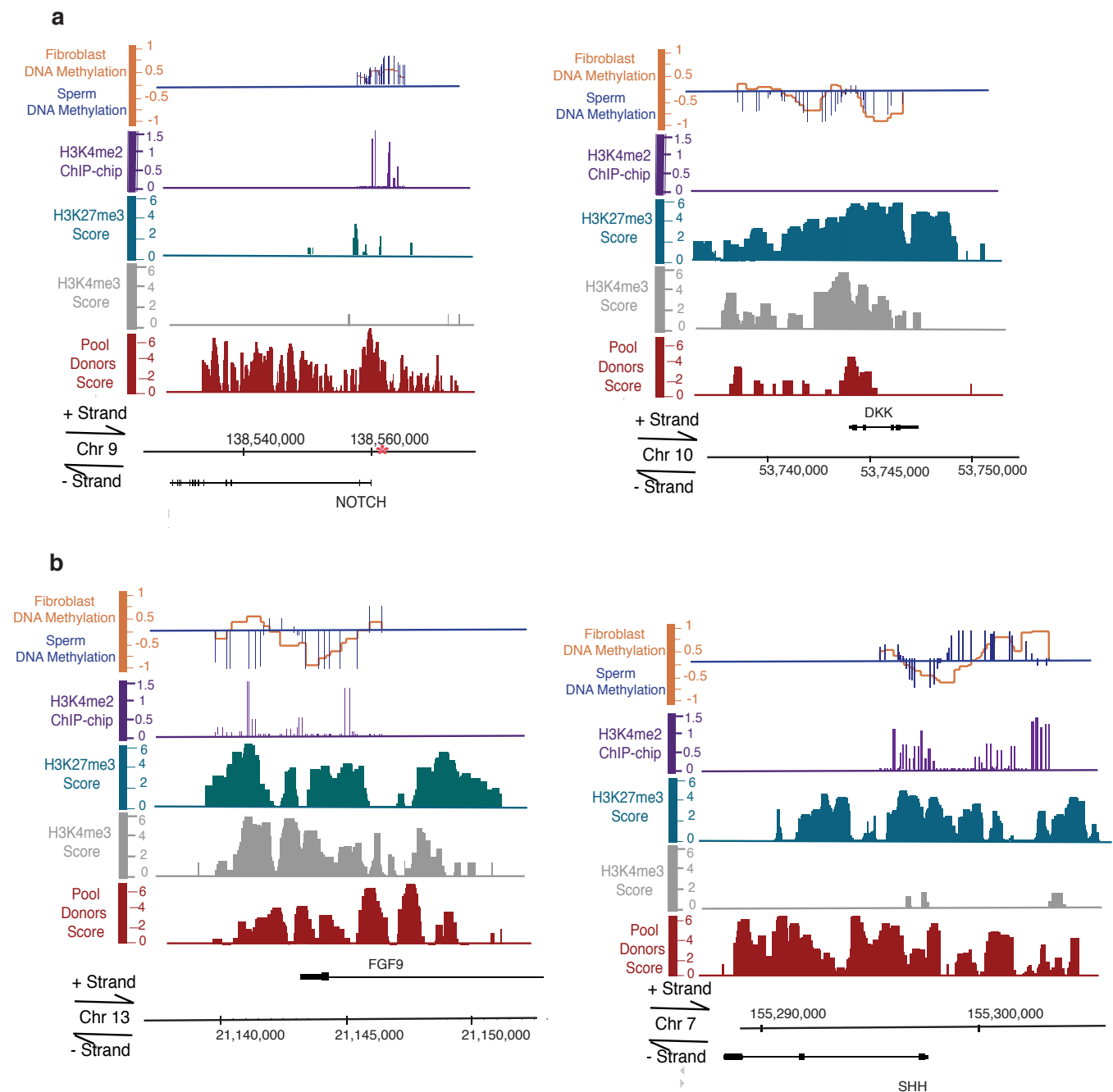
Supplemental Fig. 2: Schematic representation of experimental procedures. Two fertile donors were used for methylation studies, one donor (D1) was used for all histone modifications studied on the arrays. A pool of fertile donors were utilized for mononucleosome localization and characterization and to extend the analysis genome-wide using Illumina GAI.



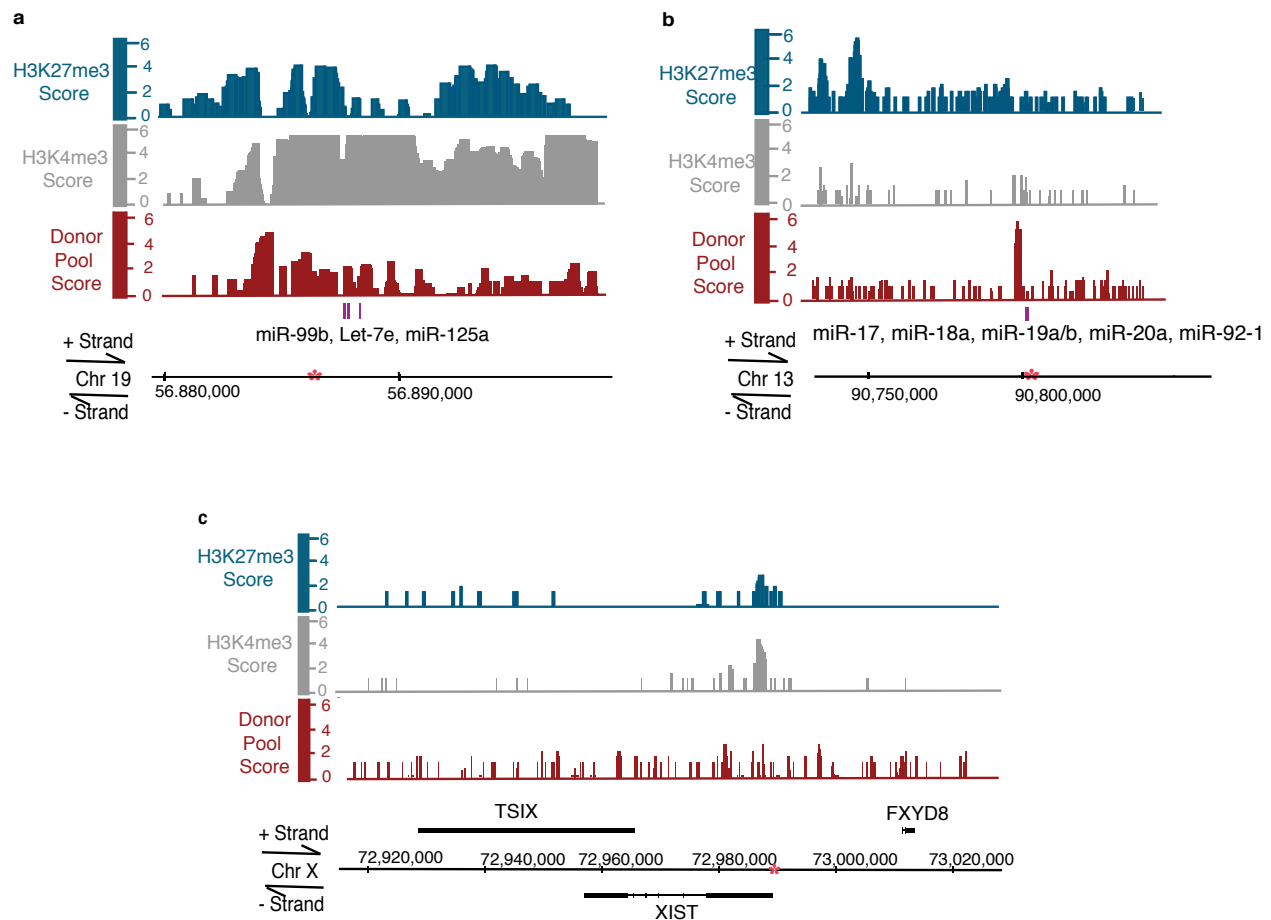
Supplemental Fig. 3: Chromatin attributes of the *HOXA*, *HOXB*, and *HOXC* loci. Histone enrichment (red bars), or histone modifications (H3K4me3 array results (ruby), H3K4me3 sequencing normalized difference scores (grey), H3K27me3 sequencing normalized difference scores (teal blue) or H3K4me2 (violet)). The y-axis is the signal intensity (log2 for array data, or normalized difference score for Illumina GAT sequencing) and the x-axis is the annotated physical map (HG18). **a**, The *HOXA* locus. **b**, The *HOXC* locus **c**, The *HOXB* locus.



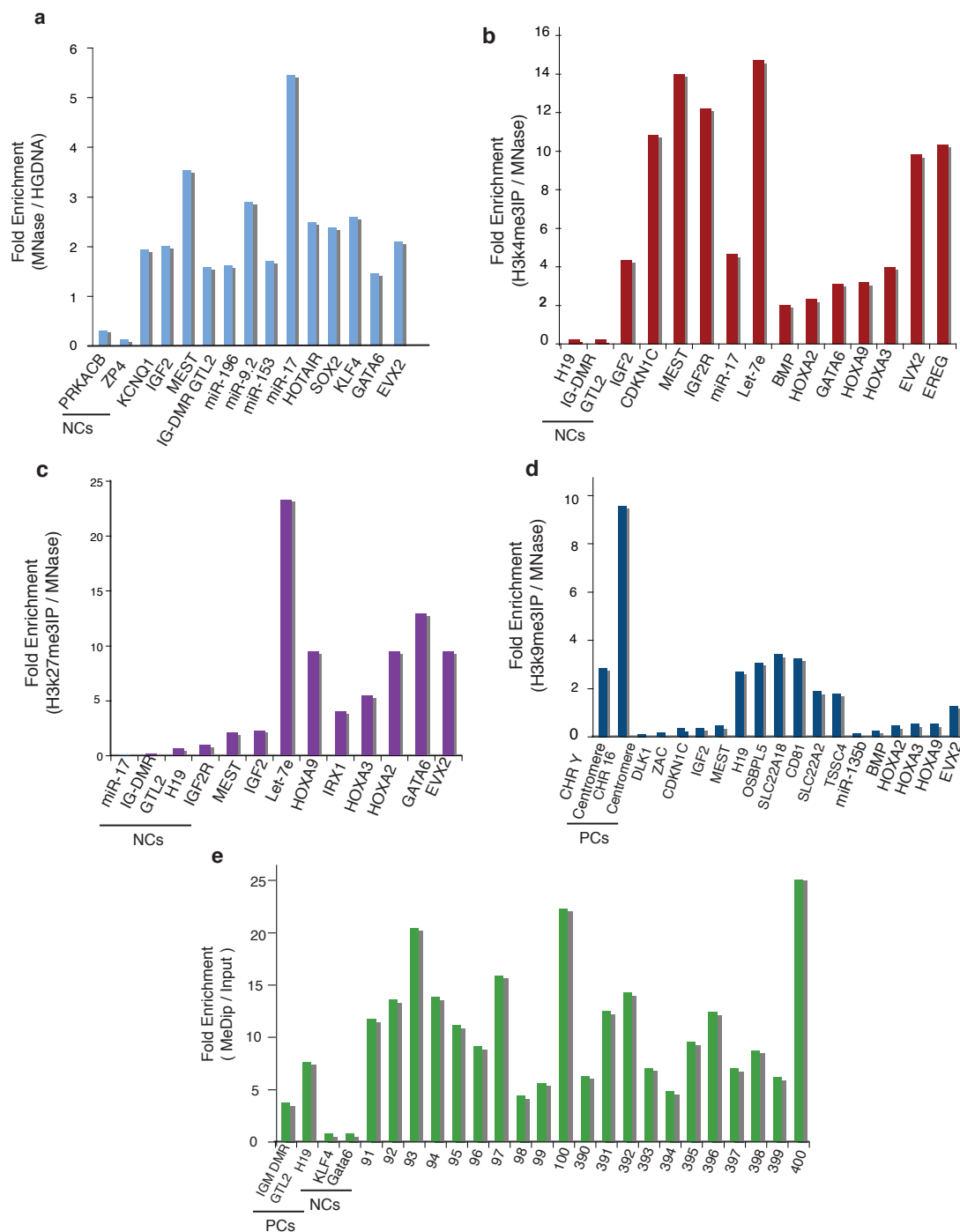
Supplemental Fig. 4: Certain self-renewal genes as well as genes required for embryonic development generally lack DNA methylation and are bivalent. **a**, *SOX2* and *FOXD3* are member of the pluripotency network. *SOX2* is demethylated and characterized by the presence of H3K4me3 and H3K27me3, whereas *FOXD3* is hypermethylated near their transcription start sites. *OCT4* and *NANOG* are also hypermethylated (Supplementary Fig. 10c). **b**, Genes involved in embryonic development are typically DNA hypomethylated, and have high levels of H3K4me2/3 and H3K27me3 around their start sites. The red asterisks indicate the region amplified for bisulfite sequencing in Supplementary Fig. 10. The y-axis is the signal intensity (log2 for ChIP-chip arrays, or normalized difference for Illumina GAII sequencing score) and the x-axis is the annotated physical map (HG18).



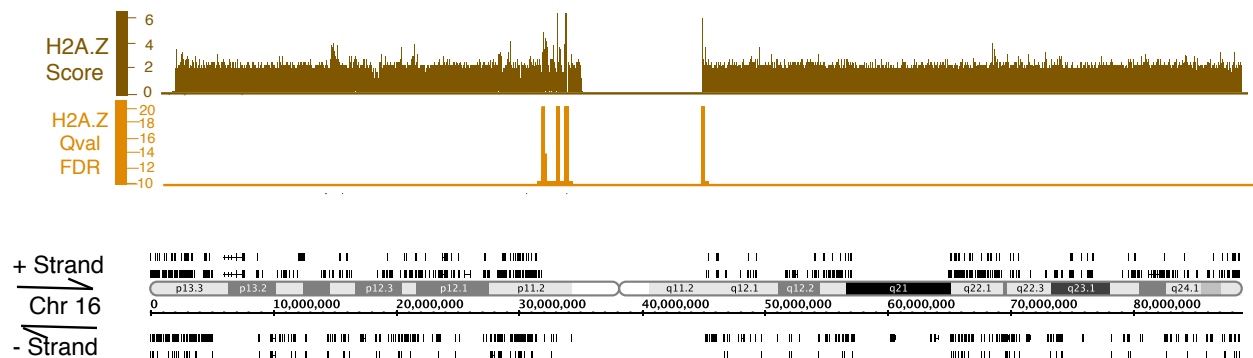
Supplemental Fig 5: Developmental and signaling factors are deficient in DNA methylation, although Notch pathway members are hypermethylated. **a**, Notch signaling pathway members, *DKK1* (hypomethylated) and *NOTCH1* (hypermethylated). **b**, FGF signaling pathway members, *FGF9* (hypomethylated) and regulator *SHH* (hypermethylated). The red asterisks indicates the region amplified for bisulfite sequencing. The y-axis is the signal intensity (log2 for ChIP-chip arrays, or normalized difference for Illumina GAI score) and the x-axis is the annotated physical map (HG18).



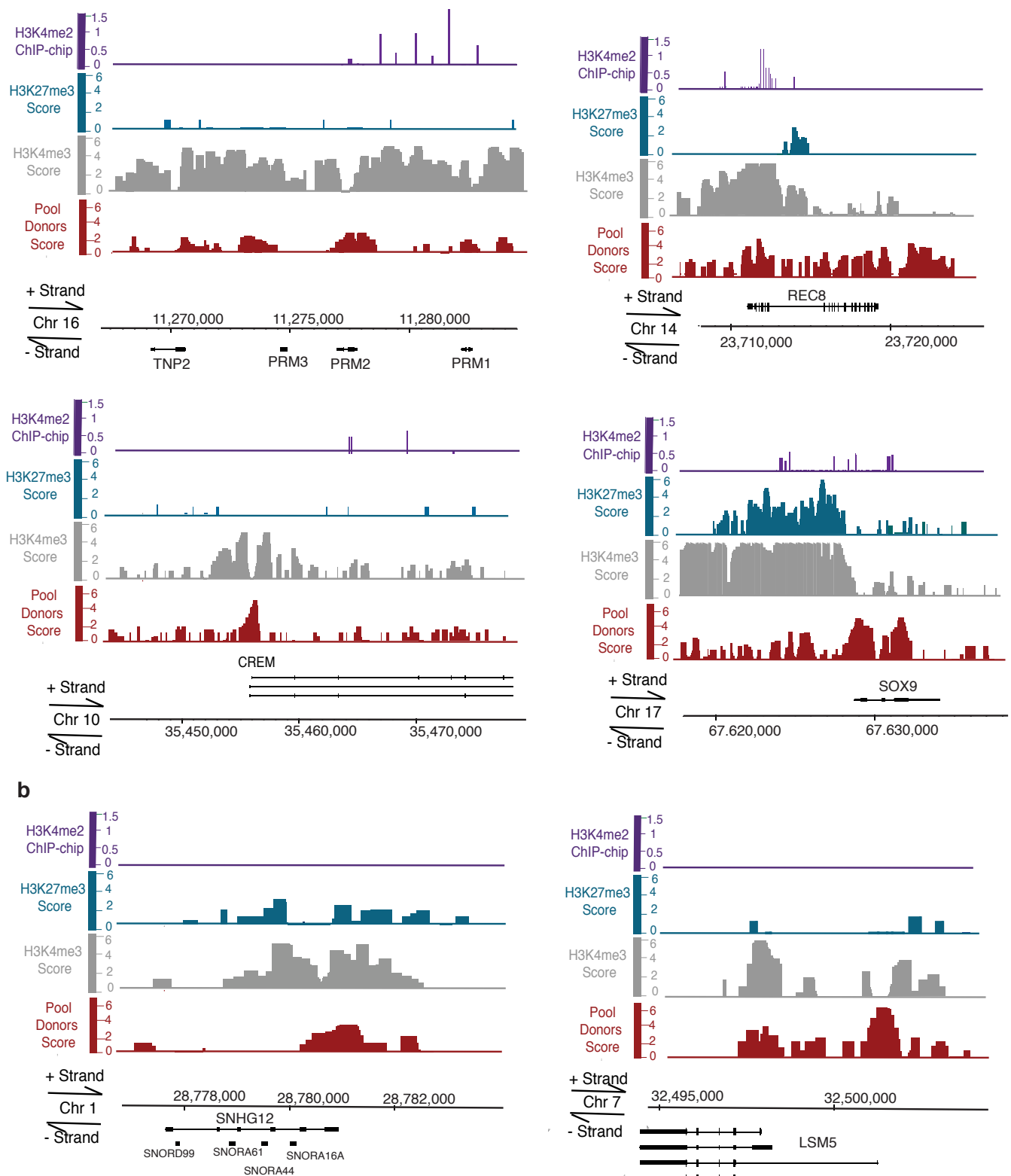
Supplemental Fig6: Histone retention at miRNAs and non-coding RNAs. **a**, A miRNA cluster with high H3K4me3 and H3K27me3. **b**, A miRNA cluster region with high levels of histone in the promoter region of the pri-miRNA, but lacking H3K4me3 and H3K27me3. **c**, The non-coding RNA *XIST* is enriched for H3K4me3 and H3K27me3 at the TSS. The read counts for the *X*-chromosome are half of those on autosomes due to the presence of either *X* or *Y* in sperm. The y-axis is the normalized difference score for sequencing. Asterisks (*) note the locations tested by bisulphite sequencing in Supplementary Fig. 10.



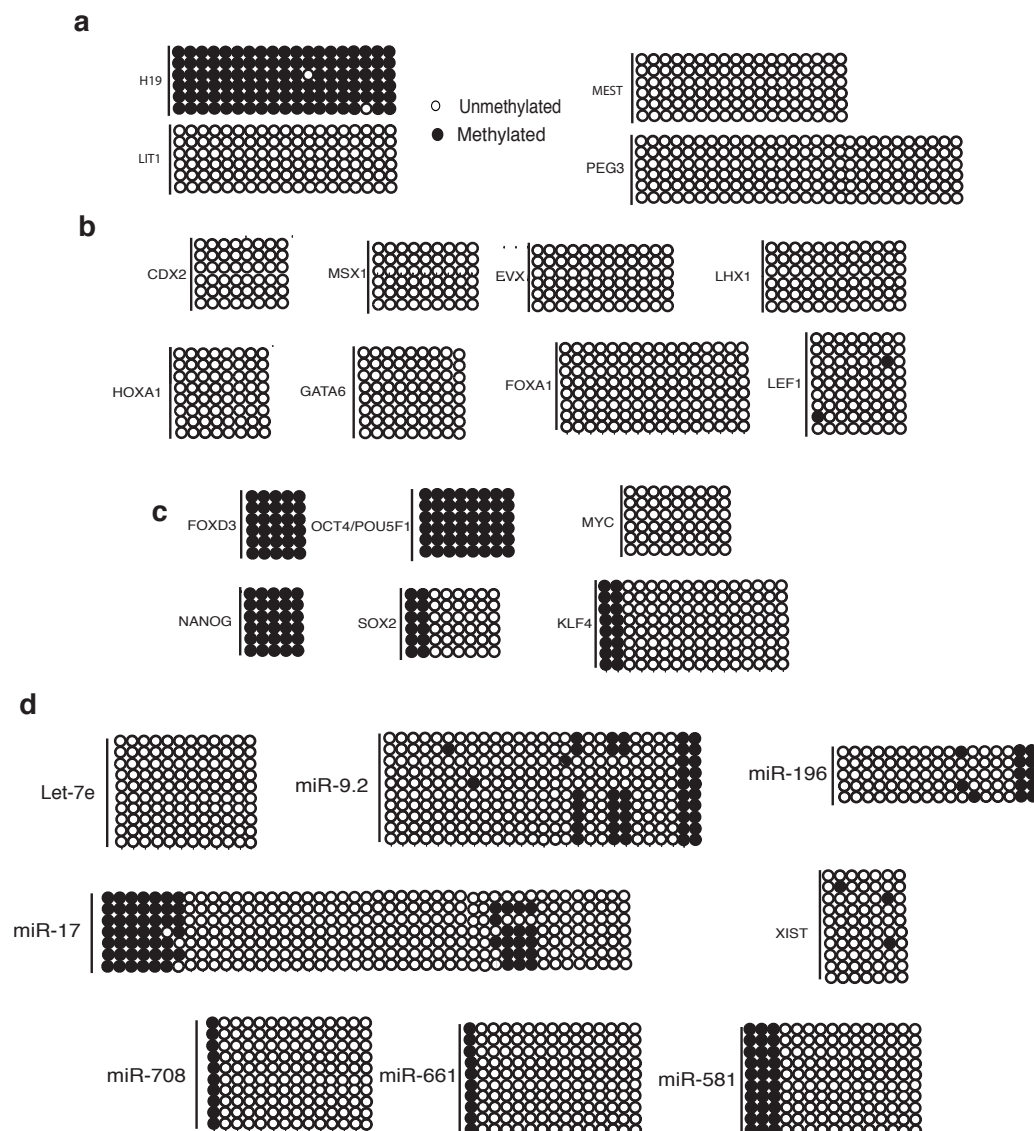
Supplemental Fig 7: qPCR testing of epigenetically modified loci enriched by Illumina GAI sequencing and/or array analysis. **a**, qPCR testing of histone occupancy at both maternally and paternally imprinted genes (*KCNQ1*, *IGF2*, *MEST*, and *IG-DMR*), miRNAs and noncoding RNA (*miR-196*, *miR-9.2*, *miR-153-1*, *miR-17*, and *HOTAIR*), and at a subset of developmental genes. Negative controls (NCs) (*PRKACB* and *ZP4*) are regions that had very low levels of histone by Illumina GAI sequencing and/or array data. Fold enrichment of histone at these promoters was determined by MNase signal divided by the total genomic DNA signal **b**, Fold enrichment of H3K4me3 was determined by normalizing signal from the H3K4me3 IP eluate to the signal from MNase (histone pool). Two maternally-imprinted loci in sperm were used as negative controls. **c**, H3K27me3 and **d**, H3K9me3 enrichment were determined as described above. H3K9me3 positive controls (PCs) were two pericentromeric heterochromatin loci. **e**, qPCR testing of MeDIP data. Enriched loci from MeDIP arrays were binned into the top 100 regions or 400 enriched regions. qPCR of MeDIP eluates were performed for the bottom 10 regions in each of the top 100 and 400 bins. Since all 20 regions enriched for DNA methylation, a cutoff of the top 400 genes (approximately 2-fold) was our stringent cutoff for DNA methylation. qPCR fold enrichment was compared to input (total sheared genomic DNA). Positive controls were two known methylated (imprinted) regions and negative controls were regions that are demethylated in sperm when compared to fibroblast.



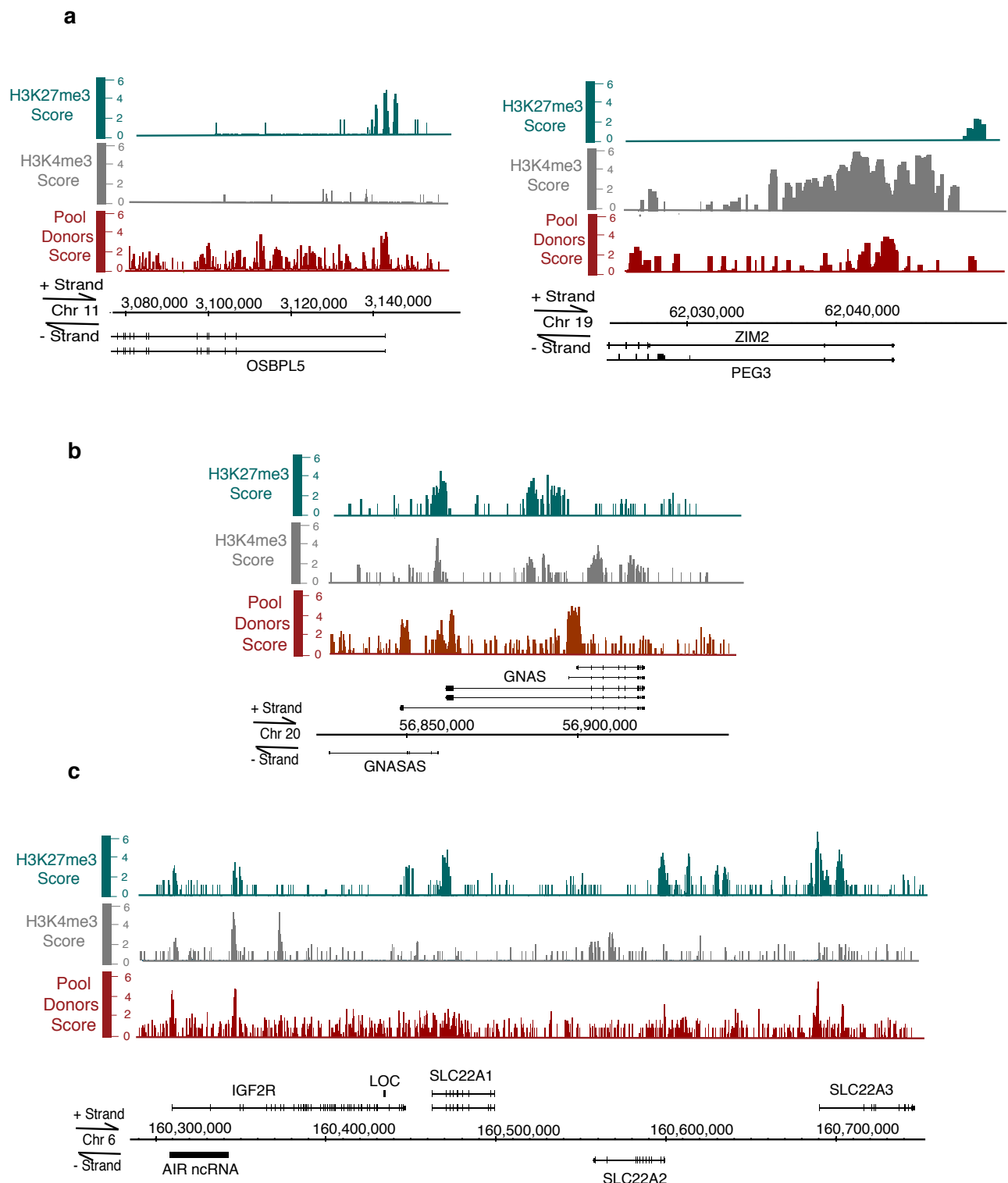
Supplemental Fig 8: H2A.Z localizes to pericentric heterochromatin in the mature human sperm. Brown bars are the normalized difference scores for pooled donor H2A.Z across chromosome 16, and in orange is the FDR. Other chromosomes showed similar peaks flanking the centromere. Pericentric heterochromatin was highly enriched with H2A.Z (FDR <0.05).

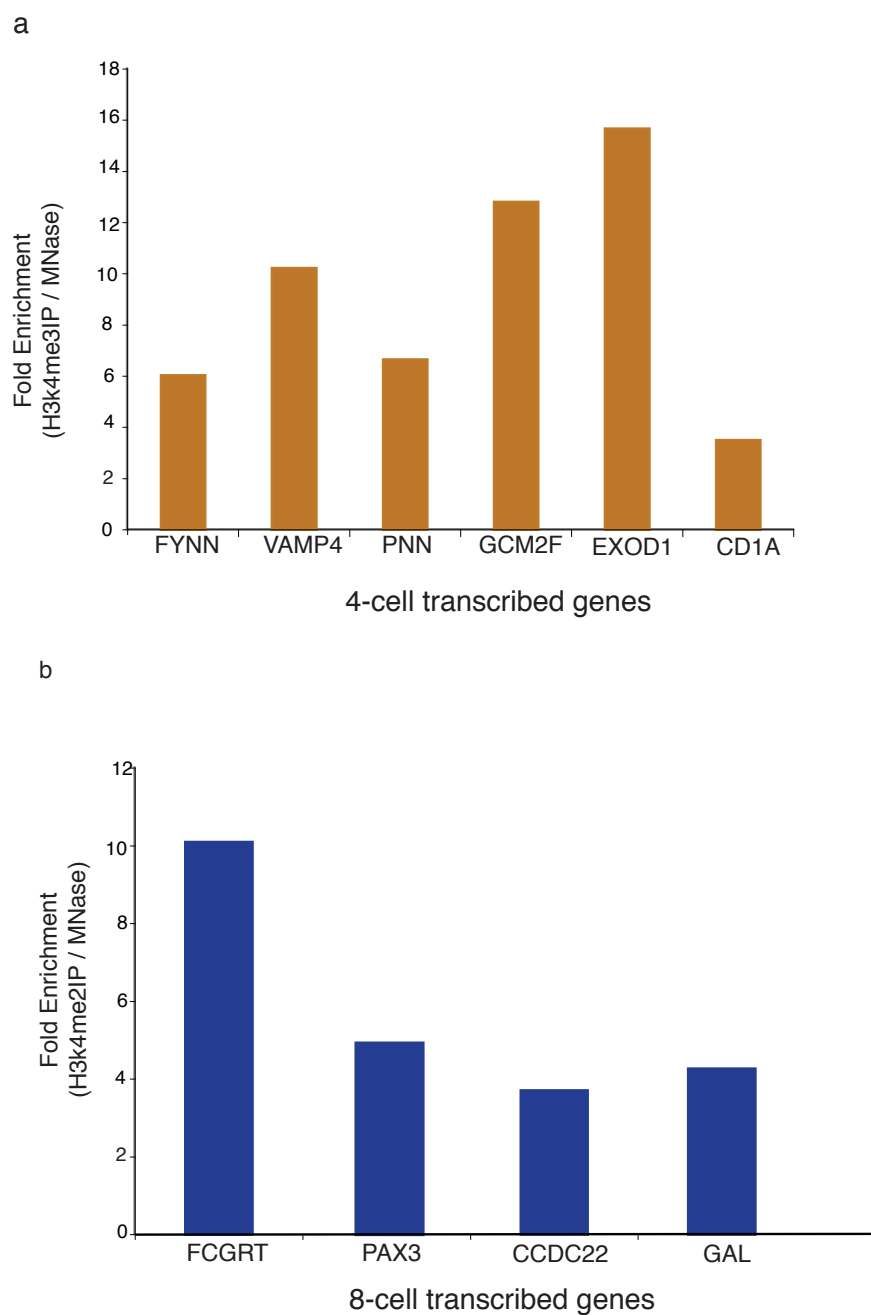


Supplemental Fig 9: Genes required for sperm development generally lack DNA methylation and are bound by H3K4me3. **a**, Four genes expressed at different stages of spermatogenesis remain DNA demethylated and retain H3K4me3 enrichment. **b**, Gene promoters involved in RNA processing, a process utilized intensely during spermiogenesis, are also demethylated and H3K4me3 bound.



Supplemental Figure 10: DNA hypomethylation at developmental promoters and miRNAs were verified by bisulfite sequencing. **a**, bisulfite sequencing of promoters known to bear (*H19*) or lack (*LIT1*, *PEG3* and *MEST*) paternal methylation in sperm chromatin. CpGs are represented as open dots (if unmethylated) or filled dots (if methylated). **b**, Hypomethylation at developmental transcription factors and **c**, a subset of the pluripotency network promoters. **d**, The TSS of the miRNAs tested were generally hypomethylated.





Supplemental Fig 12: H3K4me2/3 chromatin modifications are correlated with early embryonic genes expression at the 4 and 8 cell stage. **a**, A subset of genes enriched at the 4 cell stage have significant levels of H3K4me3 **b**, whereas genes enriched at the 8-cell stage were associated with high levels of H3K4me2. Fold enrichment for H3K4me3/2 was determined by signal from IP eluate divided the signal derived from the pooled mononucleosomes.